JACS
JOURNAL OF THE AMERICAN CHEMICAL SOCIETY

ARTICLE

pubs.acs.org/JACS

Size/Shape-Controlled Synthesis of Colloidal CdSe Quantum Disks: Ligand and Temperature Effects

Zheng Li and Xiaogang Peng*

Department of Chemistry and Biochemistry, University of Arkansas, Fayetteville, Arkansas 72701, United States

Supporting Information

ABSTRACT: Size/shape-controlled colloidal CdSe quantum disks with zinc-blende (cubic) crystal structure were synthesized using air-stable and generic starting materials. The colloidal CdSe quantum disks were approximately square, and their lateral dimensions were varied between 20 and 100 nm with the thickness controlled between 1 and 3 nm, which resulted in sharp and blue-shifted UV−vis and PL peaks due to one-dimensional quantum confinement. The quantum disks were grown with either ⟨001⟩ or ⟨111⟩ direction, polar directions in the single crystalline disks, as the short axis, and both basal planes were terminated with Cd ions. These surface Cd ions were passivated with negatively charged fatty acid ligands to neutralize the net positive charges caused by the excess monolayer of Cd ions. The coordination of the Cd ions and carboxylate groups further enabled the close-packing monolayer of fatty acid ligands on each basal plane. The close packing of the hydrocarbon chains of fatty acids dictated the up temperature limit for synthesis of the colloidal quantum disks, and the low temperature limit was found to be related to the reactivity of the starting materials. Overall, a high Cd to Se precursor ratio, negative-charged fatty acid ligands with a long hydrocarbon chain, and a proper temperature range (approximately between 140 and 250 °C) were found to be needed for successful synthesis of the colloidal CdSe quantum disks.

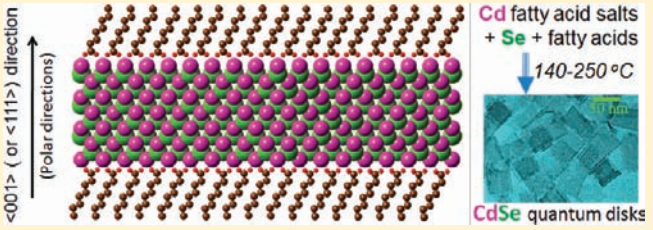

INTRODUCTION

Zero-dimensional[1,2] and one-dimensional[3] colloidal semiconductor nanocrystals, respectively known as colloidal quantum dots and quantum rods, have been successfully synthesized about 10 years ago with good control on size, shape, and size/shape distribution.[4−6] Their size/shape-dependent properties coupled with excellent solution processability are being actively explored for applications in biomedical labeling,[7,8] solar cells,[9,10] light emitting diodes,[11,12] etc. The synthesis of colloidal two-dimensional semiconductor nanocrystals with one-dimensional quantum confinement, however, has not been well established yet. After the synthesis of very thin CdSe nanoribbons was reported in 2006,[13] sheets and belts of semiconductors at least with one dimension in bulk size regime but with very small thickness showing one-dimensional quantum confinement have been reported,[14−19] but the colloidal processability/stability of those relatively large objects is usually not very good, although it was mentioned that, upon sonication, nanosheets could be temporarily dispersed into organic solvents.[15] Although several examples of semiconductor nanodisks with their lateral dimensions below 100 nm have also been reported,[20−24] the optical properties of those nanodisks typically did not demonstrate one-dimensional quantum confinement. Up to the present, the most inspiring results were reported by Dubertret's group in their 2008 communication.[25] Although the synthetic chemistry including size/shape control and characterization of the resulting nanocrystals was not well documented in Dubertret's report, CdSe nanocrystals with strong evidence of one-dimensional quantum confinement and with their lateral sizes in the order of tens of nanometers were clearly observed, which should possess good colloidal stability. The Dubertret groups' work further demonstrated that the CdSe 1D structures were in zinc-blende structure, and some interesting insights were offered on the formation of wurtzite CdSe 1D nanosheets.[15] These facts invited us to design systematic experiments to establish reproducible and mechanism-driven synthetic schemes for size/shape-controlled one-dimensional quantum confined and colloidal-stable nanostructures.

The formation mechanism of colloidal quantum rods[26,27] and quantum dots[28,29] has been extensively studied in recent years, which could shed some light on designing/refining synthetic chemistry of colloidal two-dimensional semiconductor nanocrystals. Using the most studied CdSe nanocrystal system as an example, the first requirement for formation of CdSe quantum rods is the existence of a unique axis for growth. For wurtzite and zinc blende crystal structures that are common for typical II−VI and III−V semiconductors, the polar axes conveniently acted as this role. As a result, when the monomer concentration in solution was sufficiently high, one-dimensional growth (1D-growth) occurred to form quantum rods. Formation of quantum disks, on the contrary, will need to suppress the 1D-growth. One way to substantially reduce the reactivity of the polar surfaces, more accurately, reverse the reactivity of polar surface and the other surfaces of the nanocrystals, presumably is to completely

Received: September 9, 2010
Published: April 08, 2011

dx.doi.org/10.1021/ja108145c | J. Am. Chem. Soc. 2011, 133, 6578–6586

passivate the polar surfaces of CdSe with complementary charges. In general, the synthesis of colloidal nanocrystals relies on ligands for cations only, and thus both basal planes of a quantum disk with its short axis being a polar axis should be terminated with cations, such as Cd ions for CdSe. As a result, the disk should possess an excess monolayer of cations, and the ligands should be negatively charged, such as the commonly used deprotonated fatty acids.

The hypothesis presented in the above paragraph is some sort of "soft template" approach offered by the fatty acid ligands, which would require the surface ligands to be bonded onto the basal planes of the disks quite tightly. It was observed that, however, the surface ligands on colloidal nanocrystals could only act as "soft template" when the reaction temperature is substantially low, certainly below the boiling point of a ligand in its bulk form.[30] This is understandable because high temperature would destroy the packing of ligands that is needed for the formation of any "soft template".

Therefore, combining the analysis of above two paragraphs, one could reason that two key parameters for synthesis of colloidal quantum disks should be an appropriate choice of ligands and a suited reaction temperature range for synthesis of quantum disks. In addition, a low monomer concentration to prevent the 1D-growth and a high Cd to Se ratio for the growth of CdSe disks should be other parameters to watch.

Experimental results to be described below confirmed that, within a defined temperature range, colloidal CdSe quantum disks with good control of both their thickness and their lateral dimensions can be synthesized using generic and air-stable chemicals. The hydrocarbon chain length of the fatty acids was found to dictate the up temperature limit for the formation of quantum disks. The low temperature limit was most likely determined by the activation of elemental Se in the reaction system. Characterization of the nanocrystals verified that both top and bottom basal planes of CdSe quantum disks were polar facets with Cd ions as the out layer, and these Cd surface ions were terminated with carboxylate groups of the fatty acids used in the synthesis. The single crystalline colloidal CdSe quantum disks showed very sharp UV−vis absorption and photoluminescence (PL) peaks due to one-dimensional quantum confinement. Experimental results strongly suggest that the resulting nanocrystals in the samples were quantum disks, instead of magic sized clusters.

RESULTS

The synthetic system used in this work was similar to a regular "greener" approach for the synthesis of CdSe nanocrystals using octadecene (ODE) as a noncoordinating solvent, with elemental Se as the selenium precursor and cadmium fatty acid salts as cadmium precursor.[31,32] Fatty acids, either with the same hydrocarbon chain length or a different one with the cadmium fatty acid salts, might be added as additional ligands when needed. As pointed out above, the chain length of the fatty acids from the cadmium precursor and/or the additional ligands used was a key parameter varied during the study.

It should be pointed out that several different types of cadmium fatty acid salts, such as cadmium acetate ($CdAc_2$), cadmium butanoate ($CdBu_2$), and cadmium octanoate ($CdOc_2$), were examined. Under proper conditions, all of these cadmium fatty acid salts yielded CdSe quantum disks. Furthermore, the cadmium fatty acid salts such as $CdBu_2$, $CdOc_2$, and additional corresponding fatty acid ligands also led to the formation of 1D

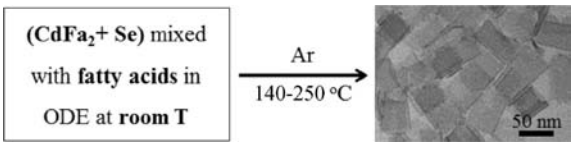

Figure 1. Reaction scheme for the synthesis of CdSe quantum disks. Here, $CdFa_2$ stands for cadmium fatty acid salts. The up reaction temperature limit depended on the fatty acids used in the system.

confined nanostructures (see Figure S1). Because of the ready availability of cadmium acetate, we concentrated on optimization of the quantum disk synthesis using this generic cadmium precursor. Studies on using cadmium fatty acid salts with different hydrocarbon chain lengths shall be the subject of future reports.

The facts mentioned in the above paragraph seemed different from what reported by the Dubertret's group.[25] They mentioned in their report that $CdAc_2$ or other types of acetates were found to be necessary for the formation of two-dimensional CdSe nanostructures.

It was known that, for formation of CdSe and other types of II−VI quantum rods, monomer concentrations must be sufficiently high to promote 1D-growth[26,27,33] and maintain the stability of the thermodynamically unstable rod shape. To study the monomer concentration effect, we varied the initial precursor concentrations in the solution. However, the results (see Figure S2) did not show noticeable difference within the precursor concentration range tested. We suspected that, because the Se powder was used directly in the synthesis without any activation reagents (see Figure 1), the active monomer concentration in the solution at the relatively low reaction temperatures employed in this work was never sufficiently high (see detail below for activation of Se precursor). Thus, future work would be needed to clarify this effect.

It was further identified that formation of CdSe quantum disks did not require any injections. In other words, all of the reactants could be mixed at room temperature and heated to a designated reaction temperature (see scheme in Figure 1). This was true for all types of cadmium fatty acid salts used. The designated reaction temperature range depended on the chain length of the fatty acids used, but generally it was between 140 and 250 °C. Detailed results for identification of the reaction temperature range will be discussed systematically later.

The one-dimensional quantum confinement of the two-dimensional quantum disks was confirmed with UV−vis and PL measurements. In Figure 2A, a typical quantum disk sample shows a significantly blue-shifted absorption band edge in comparison to that of bulk CdSe that is known to be at around 720 nm. The two sharp peaks in the UV−vis spectra could be assigned to the excitonic absorption features of a two-dimensional CdSe nanocrystal sample with the thickness being around 2 nm.[25]

Similar to the sharp UV−vis features, the PL peak of CdSe quantum disks was also sharp, with its full width at half-maximum being around 0.05 eV (8 nm). For the sample shown in Figure 2A, the PL quantum yield was found to be around 1.6%, but generally this value was observed to be extremely sensitive to the solution composition. The PL brightness was diminished by purifying away the free fatty acid ligands in the solution, indicating a relatively weak bonding of the surface ligands as expected.

Colloidal CdSe quantum disks with their UV−vis peaks at 392 and 512 nm, corresponding to thickness as around 1.6 and

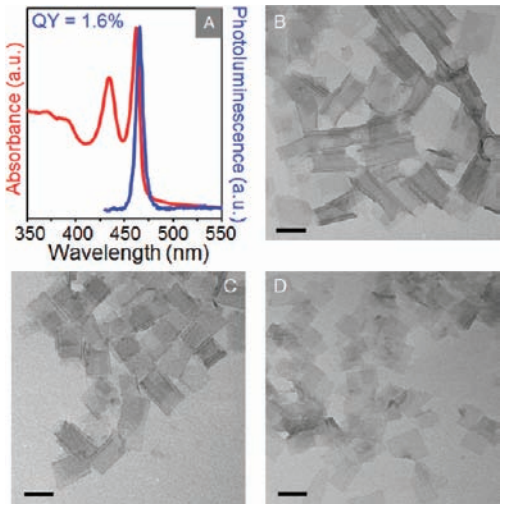

Figure 2. (A) UV−vis (red curve) and PL (blue curve) of a typical CdSe quantum disks colloidal solution. (B−D) TEM pictures of CdSe quantum disks with different lateral dimensions. Scale bar: 50 nm.

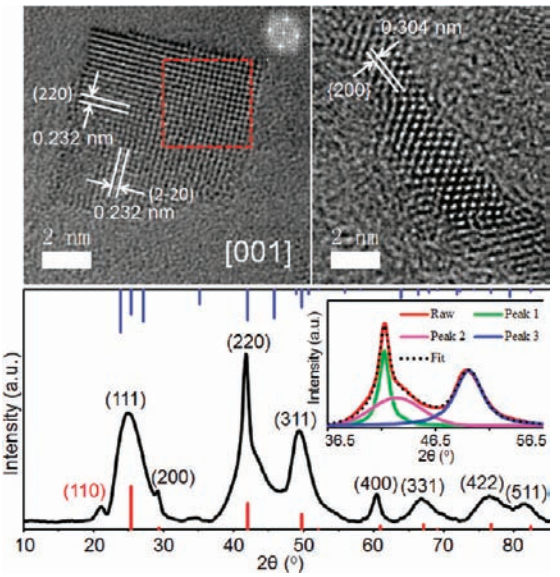

Figure 3. HRTEM image of a quantum disk (top left), side view of a quantum disk (top right), X-ray diffraction pattern of a quantum disk sample (bottom), and the peak fit results for (220) and (311) peaks (bottom, inset). In the X-ray diffraction pattern (bottom), the standard diffraction peaks for wurtzite (blue lines, JCPDS card no. 77-2307) and zinc blende (red lines, JCPDS card no. 88-2346) are inserted as references.

2.2 nm,[25] were also obtained in this study, although we concentrated on the ones with their UV−vis and PL spectra shown in Figure 2.

Size and shape control of the two-dimensional CdSe nanocrystals was achieved. The shape of colloidal CdSe quantum disks was generally controlled to be square/rectangular (see representative transmission electron microscope (TEM) images in Figure 2). When the lateral dimensions were relatively large, the quantum disks were always found to be curved along one direction (see Figure 2B and Figure S3A as an example). On the contrary, the colloidal quantum disks with small lateral dimensions (Figure 2D) would not appear to be curved on TEM images, but they intended to stack on top of each other substantially.

Thin sheets nanocrystals with their lateral dimensions above micrometers were found to be unstable as a colloidal solution in common solvents such as hexanes, toluene, chloroform, etc. The temporary suspension in nonpolar solvents typically possessed a significant scattering tail extending into near-infrared window in their UV−vis absorption spectra. Sometimes, significant light scattering could be observed with bare eyes if the nanosheets were too large. As the emphasis of this work was colloidal stable nanocrystals with one-dimensional quantum confinement, we did not study the formation of those nanosheets in detail.

The lateral dimensions of the quantum discs could be varied in the range between 20 and 100 nm, which still possessed good colloidal stability. The lateral dimensions were found to be mostly dependent on the concentration of fatty acids, the chain length of fatty acids, and the reaction temperature. A low concentration of fatty acid ligands resulted in large lateral dimensions if other reaction conditions were the same. For example, at 170 °C and in 4 g of ODE, if myristic acid concentration was 0.025 mmol, the resulting quantum disks were the largest ones in Figure 2 (Figure 2B), and when the ligand concentration was doubled, we obtained the quantum disks shown in Figure 2C. Increasing the chain length of fatty acids had an effect similar to that of increasing their concentration. For instance, the small quantum disks in Figure 2D were synthesized using 0.050 mmol of stearic acid as the ligands under the same reactions as those used for synthesizing the quantum disks in Figure 2C. As for temperature effects, a low reaction temperature typically yielded quantum disks with small lateral dimensions (see Figure S3B and C and the related caption).

The crystal structure and single-crystal nature of the colloidal quantum disks were identified using high-resolution TEM (HRTEM) and X-ray powder diffraction (Figure 3). HRTEM image in Figure 3 confirmed that the colloidal quantum disks were mostly square in shape (top left), and the thickness (top right) was similar to what was estimated from the UV−vis peak mentioned above. The corresponding Fourier transform (FT) of the red dotted area for the top view HRTEM image (top left, Figure 3) confirmed the zone axis as [001] direction of zinc blende CdSe. The side view HRTEM image (Figure 3, top right) with a quantum disk "standing up" verified the adjacent plane distance as 0.304 nm, in good accordance with the {200} plane distance in zinc blende structure. However, the {220} plane distance shown in the top view image (Figure 3, top left) was around 8% larger than the bulk value. These facts imply that there should be some distortion of the disks along different directions. It should be pointed out that, although we do not have a definite explanation for this lattice expansion, both lattice contraction[34,35] and lattice expansion[36−38] of nanoparticles were reported in the literature. Furthermore, as to be described below, the X-ray diffraction measurements also confirmed the lattice parameter difference between the {220} planes on the lateral direction and the short axis direction.

Another distinguishable feature between quantum disks and quantum dots/rods is the nonuniform lattice fringes revealed by Figure 3, especially in the top view HRTEM image. This is likely due to the combination of a very thin thickness and relatively large lateral dimensions of the quantum disks. As revealed by low resolution TEM images in Figure 2, such distortion would become even more significant as the edges of the quantum disks with large lateral dimensions curved along one direction (see Figure 2B and the related text). As a result, HRTEM experiments

dx.doi.org/10.1021/ja108145c |J. Am. Chem. Soc. 2011, 133, 6578–6586

with those quantum disks with relatively large lateral dimensions were found to be very difficult.

The growth directions of the CdSe quantum disks were determined mostly by X-ray diffraction with the support of HRTEM. From the HRTEM image shown in Figure 3 (top), one can identify that the short axis of that specific quantum disk is ⟨001⟩ direction. Based on the broad (111) peak of XRD pattern, corroborated by surveying the quantum disks under HRTEM (see Figure S4), one could also identify another short axis direction as ⟨111⟩. The best way to identify the growth direction, however, is X-ray powder diffraction as demonstrated in the case of CdSe quantum rods.[3,26,27] This is because the width of a diffraction peak increases as the dimension of the periodic arrangement along the corresponding direction (commonly known as crystalline domain size) decreases. In principle, the domain size could be calculated quantitatively using the well-known Scherrer equation if no mechanical distortion in place.

As compared to two typical reference patterns of bulk CdSe, that is, wurtzite and zinc blende structure, it is evident that the quantum disks are face-centered cubic $F\bar{4}3m$ structure, or zinc blende structure. This is consistent with the conclusion from HRTEM measurements as discussed above.

For zinc blende (cubic lattice) structure, if the short axis directions of the quantum disks were ⟨111⟩ and ⟨001⟩ axes as suggested by HRTEM experiments, ⟨110⟩ and ⟨100⟩ could be the lateral directions perpendicular to the short axis direction (Figure S5, Supporting Information). Considering the specific crystal structure, (220), (200), and (400) diffraction peaks should be the three main sharp diffraction peaks. By inspecting the diffraction pattern (Figure 3, bottom) qualitatively, one could indeed identify (220), (200), and (400) peaks as three unusually sharp peaks in the pattern.

Among the three sharp peaks, the (200) peak overlapped with the strong (111) peak and was difficult to interpret. However, inspecting the (220) and (400) diffraction peaks carefully, each of them is most likely a superposition of one broad peak and one very narrow peak. Taking the (220) as the example, two contributions could be well separated using computer peak fit with Voigt function,[39] with a narrow "peak 1" at 41.7 and a broad "peak 2" at 42.9 degree (Figure 3, bottom inset). As a comparison, the neighboring (311) peak was fitted well with a single Voigt function, "peak 3".

A single diffraction peak with two distinguishable width values for (220) is not surprising for the colloidal CdSe quantum disks reported here. This is because, as pointed out above, the colloidal quantum disks were in zinc blende crystal structure, which is a cubic lattice and possesses multiplicity of Bragg planes with the same diffraction peak. For an isotropic structure, all of these Bragg planes would overlap with each other, with the same position and same peak width. For a very thin disk, however, the Bragg planes perpendicular to the short axis would show a much narrower (200) peak than the Bragg planes parallel to the short axis.

Overall, the entire diffraction pattern shown in Figure 3 (bottom) matched well with the CdSe quantum disks with a mixture of ⟨111⟩ and ⟨001⟩ as their short axes (see more results in Figure S5 in the Supporting Information). Quantitatively, the crystalline domain size along the short axis calculated from the scherrer equation was around 2.3 nm, quite close to that estimated from UV−vis peak and TEM results (see above). The lateral dimension estimated from XRD peak width was around 12.4 nm, which seemed to be far less than the values expected (around 50 nm for this specific sample based on TEM),

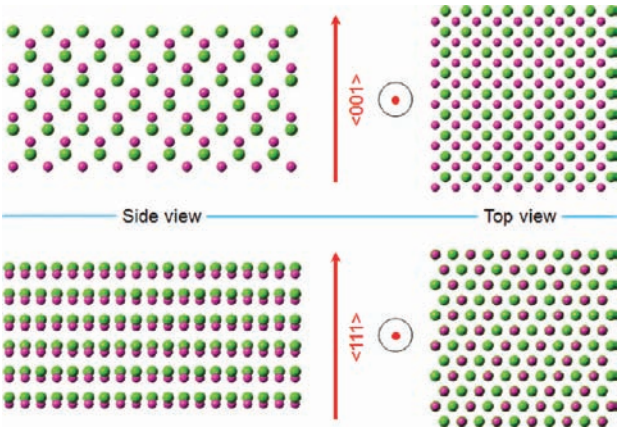

Figure 4. Schematic illustration of the atomic arrangement of CdSe zinc blende crystal with ⟨001⟩ direction (top panel) and ⟨111⟩ direction (bottom panel). The lime green and magenta balls represent Se and Cd ions, respectively.

although they were still much larger than that of the short axis dimension. This is likely due to the distortion of the lattice as observed by HRTEM. Presumably, lattice distortion would disturb the periodicity, which thus reduced the diffraction coherence. Furthermore, for those quantum discs with curved edges (see Figure 2B and C), the crystalline domain sizes along the lateral dimensions would be reduced significantly. The appearance of the forbidden (110) peak (Figure 3, bottom) is also likely due to the distortion of the lattice (see detailed analysis following Figure S6, Supporting Information).

It should be mentioned that the existence of two growth directions is not in contradictory with the optical properties of the quantum discs (Figure 2A). On the basis of the calculations (see the Supporting Information), the thickness difference along two growth directions would be extremely small, which should not lead to the appearance of distinguishable absorption and PL peaks due to different thickness.

The basal planes of the CdSe quantum disks possess one feature in common for the CdSe quantum disks with both types of short axis orientations, either ⟨111⟩ or ⟨001⟩ direction. Along ⟨111⟩ (or ⟨001⟩) direction, a usual packing scheme for a neutral crystal shall be polar, with the dipole moment oriented exactly the same as ⟨111⟩ (or ⟨001⟩) axis (Figure 4). Such dipole moment was caused by the alternating packing of Cd and Se layers along the given axis.[40,41] This means that the basic structures of the quantum disks are consistent with what was speculated in the Introduction: a quantum disk could be formed by stopping the 1D-growth along its polar axis in the lattice structure, which should thus turn a polar axis into the short axis of the disk.

The schematic packing patterns shown in Figure 4, however, reveal that only one side of the polar basal plane should be terminated with Cd for both cases if the Cd:Se ratio was 1: 1 in the quantum disks for both cases. The other basal plane opposite to the one terminated with Cd ions should be completely terminated by Se ions in such a neutral crystal (see the side view schemes in Figure 4). In fact, this structural feature was believed to be the reason why II−VI semiconductor quantum rods could be controllably synthesized under significantly higher temperatures and higher monomer concentrations through the 1D-growth mode.[27]

The hypothesis mentioned in the Introduction, however, was to passivate both basal planes of the quantum disks with organic

ligands, that is, fatty acids. This would require the control of two basic parameters. The first one is a relatively low reaction temperature to retain the ligands bonding onto the basal planes, which will be confirmed in the next subsection. The second requirement is to have an additional Cd ion layer grown onto the basal plane terminated with Se ions in Figure 4 (the top basal plane in the side view schemes, Figure 4), which should then enable the bonding of fatty acid ligands onto both basal planes.

Evidently, if the second requirement discussed in the above paragraph was realized, one would find the Cd to Se ratio significantly different from 1: 1, given that there were only a few monolayers of CdSe along the short axis directions. Energy dispersive X-ray spectroscopy (EDX) coupled with X-ray photoelectron spectroscopy (XPS) were employed to accurately identify the Cd to Se ratio in colloidal CdSe quantum disks. Three batches of carefully purified colloidal quantum disks samples were analyzed parallel with a commercial CdSe microanalysis standard (see the EDX spectra in Figure S7) using a carefully calibrated EDX setup.[42] Quantitative analysis of the commercial standard using the EDX protocol gave a Cd:Se ratio of 1.0:1.0, with an error of ±0.3% for eight different measurements for the same standard. On the contrary, the Cd:Se ratio was found to be 1.0:0.69 for the quantum disk samples, with an error being ±1.4% for 24 different measurements with three different batches of colloidal quantum disks (see detailed analysis results in Table S1).

With the thickness of the quantum disks being around 2 nm, the number of repeating CdSe atomic layers should be approximately 5 to 6 repeating layers along the thickness direction. Simple theoretical calculation using such a model gave us a Cd:Se ratio of around 1.0:0.83. Considering the imperfection of the disk structures revealed by TEM studies (Figures 2 and 3) and the simplicity of the model, we considered that the theoretical value and experimental values were in a good agreement.

The somewhat higher Cd:Se ratio in the experimental data could be a result of the residue of starting Cd precursors or oxidation products (such as CdO) formed during synthesis and purification. Under the given synthetic conditions, the Cd ions in all of these types of Cd containing compounds should have a distinguishable chemical environment in comparison to the Cd−Se bond in the quantum disks. Most likely, those Cd ions should be bonded with oxygen. XPS measurements, however, undoubtedly confirmed that all Cd ions were bonded with Se (Figure S8, Supporting Information), which excluded possible contamination of the starting materials and CdO.

A related experimental observation should be mentioned. It was found that, for the formation of good quality CdSe quantum disks, the Cd and Se precursor ratio must be substantially higher than 1: 1 (see details in the Experimental Section). Such reaction conditions are considered to be consistent with a Cd-rich product and fatty acid ligand passivation for stopping the 1D-growth along the polar axes of the nanocrystals.

The bonding nature between the ligands and the colloidal quantum disks was studied using FTIR. As shown in Figure 5, for the colloidal quantum disks formed either under typical reaction conditions or with the addition of fatty amines (the latter case to be discussed in detail later), the surface fatty acid ligands were in the form of negatively charged carboxylate ($-COO^-$) as expected. On the basis of the peak position of the asymmetric vibration of the carboxylate group, one could conclude that the bonding between the carboxylate group and the surface cadmium ions was "bridging".[43−45]

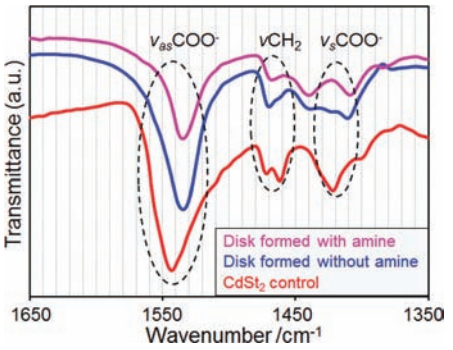

Figure 5. FTIR spectra of purified colloidal CdSe quantum disks formed with and without fatty amines added. For reference, the FTIR spectrum of cadmium stearate ($CdSt_2$) is also provided.

In comparison to the standard spectrum of cadmium stearate ($CdSt_2$), however, the asymmetric vibration band of the $-COO^-$ group shifted noticeably to lower wavenumbers (Figure 5). This indicates that, in comparison to the standard bonding of free cadmium ions and deprotonated fatty acids, the carboxylate ligands bonded somewhat weaker to the surface Cd ions.

It should be pointed out that, for reaction with amine in place, the concentration of the fatty amines could be several times higher than that of fatty acids. However, after careful purification, there was no sign of fatty amines in the IR spectrum of the colloidal quantum disks samples (see Figure S9 for more details, Supporting Information), although it is well-known that both amines and fatty acids are common ligands for CdSe nanocrystals. This strongly supports the hypothesis that the negatively charged carboxylate groups from the fatty acid ligands were needed to balance the charge of the CdSe quantum disks with an excess layer of Cd on one of the basal planes.

Magic sized nanoclusters have been considered a possible explanation for the sharp UV−vis and PL spectra similar to those shown in Figure 2A,[46,47] and to our understanding, the debate has not been well resolved. On the basis of the characterization results discussed above, magic sized nanoclusters could be excluded in our samples. For example, the X-ray diffraction patterns and the TEM images must be associated with quantum discs, instead of those tiny magic sized nanoclusters. Especially, the X-ray powder diffraction was performed with ensemble of the products, which offers strong evidence to exclude magic sized nanoclusters. The size of the magic sized nanoclusters should be around 2 nm to yield UV−vis and PL spectra similar to those in Figure 2A. Such tiny nanoclusters should only show extremely broad diffraction peaks,[48] and it would thus be very difficult to explain the sharp diffraction features in Figure 3 (bottom panel).

To further exclude the contamination of magic sized nanoclusters, a systematic purification procedure was developed (see details in the Experimental Section). The general chemistry wisdom tells that molecular interaction for two molecules, in this case, nanoparticles, strongly depends on their size and the distance between the center of mass points of two molecules. Thus, the face−face interaction for quantum disks should be much stronger than that between magic sized nanoclusters. Similar to size selective precipitation for size sorting of spherical nanocrystals,[1] the quantum disks should be much easier to be precipitated out from their colloidal solution.

For the reasons described above, centrifugation of a stable quantum disks solution was designed as a central step in

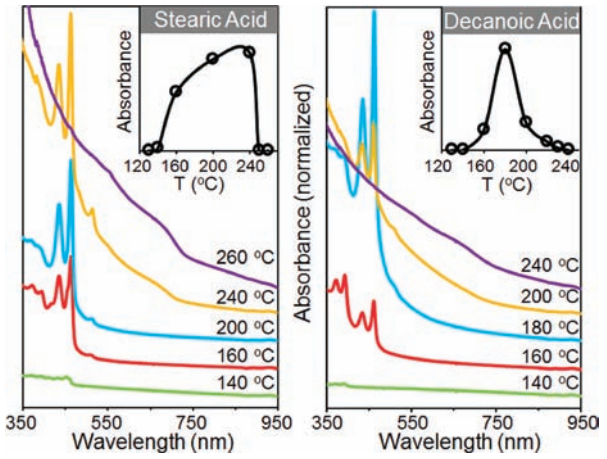

Figure 6. Temperature-dependent UV−vis spectra of the nanocrystals synthesized using stearic acid (left) and decanoic acid (right). The reaction time for all cases was fixed to be 30 min, and the UV−vis spectra were all normalized to the concentration. The inset in each series plots the absorbance of the first UV−vis peak at 462 nm versus the reaction temperature after background correction (see text for details).

purification. The nanocrystals dispersed in the ODE could be precipitated by a regular benchtop centrifuge (at 3000 rpm for 5 min). The precipitate could be completely dispersed back into a nonpolar solvent and form a stable colloidal solution. UV−vis measurements (Figure S10) revealed that at least 99.9% of the optical density was recovered in the redispersed solution and the supernatant only showed negligible UV−vis signal similar to those in Figure 2A. According to the analysis in the above paragraph, this set of experiments indicates that the nanocrystals given the sharp UV−vis and PL spectra were largely sized and could be reversibly precipitated from the colloidal solution, which should thus be the colloidal quantum disks.

It should be further mentioned that all measurements discussed in this work except those mentioned specifically were all performed with the products purified using the procedure in the Experimental Section, which further support the conclusion that the resulting nanocrystals in this work were colloidal quantum disks without contamination of the magic sized nanoclusters. In fact, if the samples were not purified, some nanoparticles were often observed under TEM along with the two-dimensional nanostructures (Figure S11), which might cause some confusion in interpretation of the experimental results. However, those particulate impurities did not show any optical activities as mentioned above and could be removed readily using the purification procedure (see the Experimental Section).

Temperature dependence for the formation of quantum disks was studied for fatty acids ligands with different chain length. Figure 6 shows two series of such reactions. The spectra series on the left is for the nanocrystals synthesized with stearic acid as ligands, and the one on the right is for the nanocrystals synthesized using decanoic acid as the ligands. To illustrate the temperature effect directly, the absorbance at 462 nm of the quantum disks normalized with the reaction mixture volume was plotted as an inset for both series with the reaction temperature as the *x*-axis (Figure 6, insets). The normalized absorbance of the UV−vis peak at 462 nm for a sample was calculated by removing the background for those relatively high temperature reactions (see Figure S12, Supporting Information).

For both cases shown in Figure 6, the formation of the quantum disks did not appear when the temperature was 140 °C and below. The formation rate of the quantum disks picked up rapidly as the reaction temperature was higher than this low temperature limit, 140 °C. Simultaneously, as the reaction temperature was higher than a certain level, formation of regular nanocrystals, under TEM, they appeared to be irregular in shape and sizes, with broad absorption features started to show up (see 240 °C reaction for the stearic acid series and 180 °C reaction for the decanoic acid series in Figure 6). When the temperature was higher than an up limit, the formation of those irregular nanocrystals dominated the formation of quantum disks (see the 260 °C reaction for the stearic acid case and the 240 °C reaction for decanoic acid case in Figure 6 and Figure S13, Supporting Information), which gave the up limit temperature for each reaction series.

The low temperature limit shall be discussed separately later. As expected, the up temperature limit was found to increase as the chain length of the fatty acids increased (Figure 6). Consequently, the temperature for appearance of those irregular nanocrystals was significantly earlier for the decanoic acid series. In addition, the maximum absorbance for the quantum disks was 180 °C for the decanoic acid series and 240 °C for the stearic acid one. This indicates that, although the hydrocarbon chain did not participate in the surface bonding, it greatly influenced the thermal stability of the two-dimensional nanostructures, which is consistent with "soft-template" growth mechanism as speculated in the Introduction.

Although the temperature achieving the maximum absorbance of the colloidal quantum disks was found to be lower than the boiling point (b.p.) of corresponding fatty acid, it was substantially higher than its melting point (m.p.) temperature. On the contrary, formation of high-quality CdSe quantum dots could be achieved in a temperature range slightly higher than the boiling point of a ligand.[30] This is again consistent with the "soft-template" mechanism proposed.

The low temperature limit for formation of the quantum disks was found to be related to the reactivity of the precursors under the reaction temperature range studied. As pointed out above, for the reaction series shown in Figure 6, the low temperature limit for both series was approximately the same, that is, ∼140 °C, although the temperature dependence pattern was sensitive to the chain length of the fatty acids.

Experiments were performed to confirm the relationship between the low temperature limit for the formation of the colloidal quantum disks and the reactivity of the precursors. Evidence revealed that fatty amines could activate the formation of chalcogenides nanocrystals when elemental chalcogens were used directly.[49] This led us to add fatty amines into the reaction system and inspect the response of the low temperature limit for formation of the colloidal quantum disks.

The results in Figure 7 (top) clearly indicate that formation of two-dimensional quantum disks was possible at 120 °C if a significant amount of oleylamine was added into the reaction system. On the contrary, under the same reaction conditions except no amine in the reaction system, the control experiment did not show any sign of reaction for the same reaction duration. It should be pointed out that, if no long chain fatty acids were in the reaction system, formation of quantum disks would not occur for the reactions with amine added (Figure 7, bottom). The experimental results revealed that the resulting nanocrystals would be quantum dots for the reaction only with fatty amines

dx.doi.org/10.1021/ja108145c |*J. Am. Chem. Soc.* 2011, 133, 6578–6586

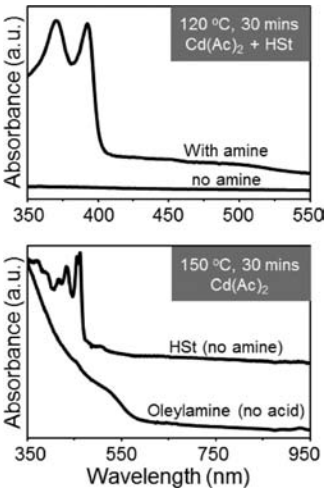

Figure 7. The effects of fatty amine on the low temperature limit for the formation of CdSe quantum disks (top), and demonstration of insufficiency of fatty amine on the formation of CdSe quantum disks (bottom).

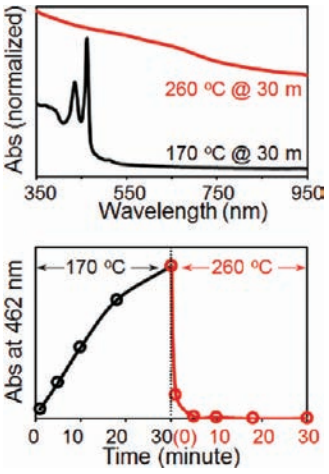

Figure 8. Thermal stability of the CdSe quantum disks at 170 and 260 °C.

but without any long chain fatty acids added. Furthermore, as described above (see Figure 5 and the related text), the surface ligands of the CdSe quantum disks were identified as pure fatty acids for the reactions with both fatty amines and fatty acids in place.

The experimental results shown in Figure 7 (bottom) not only excluded the possibility of fatty amines as ligands for the formation of CdSe quantum disks, but also imply that the existence of long chain fatty acids would be necessary for the formation of the quantum disks. On the contrary, given that the precursor for both reactions in Figure 7 (bottom) was cadmium acetate, acetates were likely too short to be the ligands for stabilization of the basal planes of the quantum disks. This observation is distinctively different from what was reported by the communication published by Dubtret's group, which speculated that the acetate group should be necessary for the formation of two-dimensional CdSe nanostructures.[25]

The thermal stability of the colloidal CdSe quantum disks was briefly examined in the reaction solutions to further identify the nature of up temperature limit for formation of quantum discs.

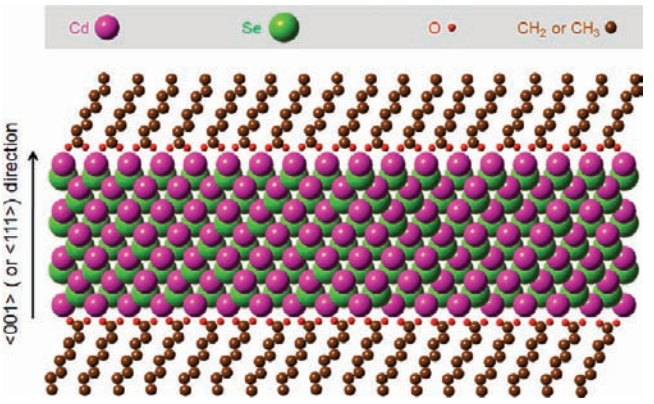

Figure 9. Schematic illustration of the colloidal CdSe quantum disk formed through the synthetic scheme shown in Figure 1.

To do so, a sample of CdSe quantum disks was synthesized using the typical procedure at 170 °C, and the reaction solution stayed at this temperature for 30 min in total. As expected, the formation of CdSe quantum disks occurred, indicated by the appearance of sharp absorption peaks as shown in Figure 8 (top). At this temperature, a gradual intensity increase of the UV−vis absorption peaks associated with the quantum disks was also observed (Figure 8, bottom).

The reaction solution containing quantum disks was subsequently heated to 260 °C rapidly and held at this temperature for 30 min, which is slightly higher than the up temperature limit for this type of quantum disks (see Figure 6 left and the related text). As shown in Figure 8, the quantum disks formed at 170 °C were completely destroyed at 260 °C, indicated by the featureless absorption spectrum (Figure 8, top). In fact, the destruction of the quantum disks was rather fast at this temperature. As shown in Figure 8 (bottom), the absorbance of the first excitonic absorption peak of the quantum disks disappeared within 5 min of heating at 260 °C.

The experimental results described in this subsection indicate that the up temperature limit should be an intrinsic temperature limit for the stability of the quantum disks, instead of a kinetic temperature limit occurred in the growth of the quantum disks. One possible explanation would be that the fatty acid ligand monolayer on the basal planes became unstable at this temperature, which subsequently caused the destruction of the quantum disks.

DISCUSSION

The experimental results described above are consistent with the hypothesis that formation of colloidal CdSe quantum disks was a result of suppression of 1D-growth along the polar directions, that is, either ⟨111⟩ or ⟨001⟩ direction, of the zinc blende lattice. These two directions are the polar axes for the structure, which enabled an alternating packing pattern of Cd and Se layers along the short axis of the quantum disks (Figure 4). Suppression of 1D-growth was made possible by terminating both basal planes of the quantum disks with a layer of Cd ions, which were passivated with deprotonated fatty acid ligands. The positive charges caused by the excess layer of Cd ions on the basal planes of each quantum disk were compensated with the negatively charged carboxylate groups of fatty acid ligands (Figure 9).

The thermal stability of such an inorganic−organic assembled nanostructure should be dominated by the relatively weak part of the entire structure, the hydrocarbon monolayer of the fatty acids

dx.doi.org/10.1021/ja108145c |J. Am. Chem. Soc. 2011, 133, 6578–6586

on both basal planes of a quantum disk. As a result, the growth of colloidal quantum disks would not occur if the temperature was above the up temperature limit for the close packing (Figure 9), which is consistent with the "soft template" growth mechanism.[30]

The bonding geometry between the fatty acid ligands and the surface Cd ions on the basal planes of the colloidal quantum disks, as described above, was the common "bridging" coordination between two Cd ions and a carboxylate group of deprotonated fatty acids (Figure 9). This bonding could have several different functions for the inorganic−organic assembly. First, it helped to saturate the surface dangling bonds of the Cd ions, which resulted in good PL properties of the quantum disks in solution (Figure 2A). Second, it could balance the positive charges of the excess Cd ions on a CdSe quantum disk with the negative charges of the carboxylate groups of the deprotonated fatty acid ligands. Third, it anchored the surface fatty acid ligands onto the relatively flat basal planes of the colloidal quantum disks, which in turn resulted in a reasonable spatial arrangement for an enhanced packing of the hydrocarbon chains of the fatty acid ligands needed for stability of the inorganic−organic nanostructures.

EXPERIMENTAL SECTION

Materials. Cadmium acetate dihydrate (Alfa), stearic acid (Alfa), decanoic acid (Avocado), oleic acid (Aldrich), octanoic acid (Alfa), oleylamine (Aldrich), myristic acid (Alfa), selenium (Alfa), 1-octadecene (ODE, Alfa), tributylphosphine (TBP, Alfa), CdSe Microanalysis Compound Standards (EMS), ethanol (Pharmco), methanol (EM Science), hexanes (EM Science), chloroform (EM Science), acetone (EM Science), and toluene (Mallinckrodt) were used without further purification.

The synthesis of CdSe quantum disks was carried out as follows. For a typical reaction, 0.0533 g of cadmium acetate dihydrate (0.20 mmol), 0.0040 g of selenium (0.05 mmol), 0.0142 g of stearic acid (0.05 mmol), and 4.0 g of ODE were heated to the designated temperature under Ar flow, and small aliquots were taken out at different time intervals, diluted in toluene, and measured by UV−vis to monitor the reaction. The total amount of quantum discs from one synthesis reaction was on the milligram scale.

Examples of quantum disks with different lateral dimensions were synthesized with different chain length/concentration of fatty acid and reaction temperature. For instance, 0.0533 g of cadmium acetate dihydrate (0.20 mmol), 0.0040 g of selenium (0.05 mmol), 0.0057 g of myristic acid (0.025 mmol), and 4.0 g of ODE were heated to 170 °C and reacted for 30 min, corresponding to Figure 2B; 0.0533 g of cadmium acetate dihydrate (0.20 mmol), 0.0040 g of selenium (0.05 mmol), 0.0114 g of myristic acid (0.05 mmol), and 4.0 g of ODE were heated to 170 °C and reacted for 30 min, corresponding to Figure 2C; 0.0533 g of cadmium acetate dihydrate (0.20 mmol), 0.0040 g of selenium (0.05 mmol), 0.0142 g of stearic acid (0.05 mmol), and 4.0 g of ODE were heated to 170 °C and reacted for 15 min, corresponding to Figure 2D. For lower temperature synthesis, more details were provided in Figure S3 and the related caption.

The synthesis of CdSe quantum disks with the addition of oleylamine under low temperatures was carried out in the following way. Cadmium acetate dihydrate (0.0533 g, 0.20 mmol), 0.0040 g of selenium (0.05 mmol), 0.0142 g of stearic acid (0.05 mmol), 0.05 g of oleylamine (0.19 mmol), and 3.95 g of ODE were mixed together and then heated to 120 °C under Ar protection. Small aliquots were taken out at different time intervals, and diluted in toluene and measured by UV−vis to monitor the reaction.

The PL QY of CdSe quantum disks was measured by comparing fluorescence intensity of coumarin 460 in ethanol[50] with CdSe quantum disks in toluene, with the same absorbance value at excitation wavelength (333 nm) and similar fluorescence wavelength.

Purification of CdSe Quantum Disks for Different Measurements. Purification of CdSe quantum disks was generally carried out by the following procedure: A TBP and EtOH mixture (10% volume ratio of TBP) was added into the final products, sonicated, then centrifugated at 14 000 rpm for 15 min, precipitate was preserved, and this was repeated for another two times. The purified samples were dissolved into toluene or hexanes, forming a clear solution.

Purification of CdSe quantum disks for XRD characterization was the same as the aforementioned procedure except that centrifugation was carried out at 3000 rpm for 15 min, EtOH was used to wash the precipitate one more time, and the final precipitate was preserved and dried in a vacuum oven overnight before grinding in mortar for XRD analysis.

Purification of CdSe quantum disks for EDX analysis was carried out by the general procedure except for the following difference: the centrifugation was carried out at 14 000 rpm for 5 min. The samples were first centrifugated to separate quantum disks from the solvent, and then the supernatant was decanted. Also, EtOH was applied to wash the samples for another three times. Final products were dried in a vacuum oven overnight before being applied to the conducting tape for EDX analysis.

Purification of CdSe quantum disks for FT-IR analysis was carried out by the following procedure: the samples were centrifugated at 14 000 rpm for 15 min to separate quantum disks from the solvent, and the supernatant was decanted. Precipitate was dissolved into hexanes, methanol was added into the solution, and an analog vortex mixer was used to enhance extraction efficiency. The solution was set aside until forming separated layers, the hexanes layer was carefully separately from the methanol layer, and the hexanes layer was centrifugated at 14 000 rpm for 15 min. The supernatant was then decanted, and the precipitate was dissolved into hexanes.

Optical Measurements. UV−vis spectra were taken on an HP 8453 UV−visible spectrophotometer. Photoluminescence spectra were measured using a Spex Fluorolog-3 fluorometer.

Transmission Electron Microscopy (TEM) and High-Resolution TEM (HRTEM). TEM images were taken on a JEOL X-100 electron microscope using a 100 kV accelerating voltage. High-resolution TEM images were taken on Fei Titan 80-300 microscope with an accerlating voltage of 300 kV. Purified CdSe quantum disks were dispersed into toluene or hexanes solution, then several drops of the solution were added onto a Formvar-coated or carbon film copper grid, and the grid with the nanocrystals was dried in air.

Fourier Transform Infrared Spectroscopy (FTIR). FTIR spectra were recorded on a Bruker Tensor 27 FT-IR spectrometer at room temperature by directly applying sample onto a KBr salt plate.

X-ray Powder Diffraction (XRD). XRD patterns were acquired using Philips PW1830 X-ray diffractometer operating at 45 kV/40 mA and a Rigaku MiniFlex X-ray diffractometer operating at 30 kV/15 mA.

Energy-Dispersive X-ray Spectroscopy (EDX). EDX was used for elemental analysis using a Philips ESEM XL30 scanning electron microscope equipped with a field emission gun and operated at 30 kV.

X-ray Photoelectron Spectroscopy (XPS). XPS spectra were obtained on a PHI 5000 VersaProbe instrument.

ASSOCIATED CONTENT

Supporting Information. Complete ref 15, additional TEM images, atomic models, XRD, EDX, XPS, FT-IR, and UV−vis data. This material is available free of charge via the Internet at http://pubs.acs.org.

AUTHOR INFORMATION

Corresponding Author
xpeng@zju.edu.cn

ACKNOWLEDGMENT

Financial support from the National Science Foundation is acknowledged. We are grateful for the enlightening discussion with Prof. Werner Massa at Philipps University.

REFERENCES

(1) Murray, C. B.; Norris, D. J.; Bawendi, M. G. *J. Am. Chem. Soc.* **1993**, *115*, 8706.
(2) Peng, Z. A.; Peng, X. G. *J. Am. Chem. Soc.* **2001**, *123*, 183.
(3) Peng, X. G.; Manna, L.; Yang, W. D.; Wickham, J.; Scher, E.; Kadavanich, A.; Alivisatos, A. P. *Nature* **2000**, *404*, 59.
(4) Murray, C. B.; Kagan, C. R.; Bawendi, M. G. *Annu. Rev. Mater. Sci.* **2000**, *30*, 545.
(5) Yin, Y.; Alivisatos, A. P. *Nature* **2005**, *437*, 664.
(6) Peng, X. G. *Nano Res.* **2009**, *2*, 425.
(7) Bruchez, M.; Moronne, M.; Gin, P.; Weiss, S.; Alivisatos, A. P. *Science* **1998**, *281*, 2013.
(8) Chan, W. C. W.; Nie, S. M. *Science* **1998**, *281*, 2016.
(9) Greenham, N. C.; Peng, X. G.; Alivisatos, A. P. *Phys. Rev. B* **1996**, *54*, 17628.
(10) Huynh, W. U.; Dittmer, J. J.; Alivisatos, A. P. *Science* **2002**, *295*, 2425.
(11) Colvin, V. L.; Schlamp, M. C.; Alivisatos, A. P. *Nature* **1994**, *370*, 354.
(12) Coe, S.; Woo, W. K.; Bawendi, M.; Bulovic, V. *Nature* **2002**, *420*, 800.
(13) Joo, J.; Son, J. S.; Kwon, S. G.; Yu, J. H.; Hyeon, T. *J. Am. Chem. Soc.* **2006**, *128*, 5632.
(14) Tang, Z. Y.; Zhang, Z. L.; Wang, Y.; Glotzer, S. C.; Kotov, N. A. *Science* **2006**, *314*, 274.
(15) Son, J. S.; et al. *Angew. Chem., Int. Ed.* **2009**, *48*, 6861.
(16) Lee, A.; Coombs, N. A.; Gourevich, I.; Kumacheva, E.; Scholes, G. D. *J. Am. Chem. Soc.* **2009**, *131*, 10182.
(17) Srivastava, S.; Santos, A.; Critchley, K.; Kim, K. S.; Podsiadlo, P.; Sun, K.; Lee, J.; Xu, C. L.; Lilly, G. D.; Glotzer, S. C.; Kotov, N. A. *Science* **2010**, *327*, 1355.
(18) Schliehe, C.; Juarez, B. H.; Pelletier, M.; Jander, S.; Greshnykh, D.; Nagel, M.; Meyer, A.; Foerster, S.; Kornowski, A.; Klinke, C.; Weller, H. *Science* **2010**, *329*, 550.
(19) Liu, Y. H.; Wayman, V. L.; Gibbons, P. C.; Loomis, R. A.; Buhro, W. E. *Nano Lett.* **2010**, *10*, 352.
(20) Sigman, M. B.; Ghezelbash, A.; Hanrath, T.; Saunders, A. E.; Lee, F.; Korgel, B. A. *J. Am. Chem. Soc.* **2003**, *125*, 16050.
(21) Park, K. H.; Jang, K.; Son, S. U. *Angew. Chem., Int. Ed.* **2006**, *45*, 4608.
(22) Acharya, S.; Sarma, D. D.; Golan, Y.; Sengupta, S.; Ariga, K. *J. Am. Chem. Soc.* **2009**, *131*, 11282.
(23) Choi, J.; Kang, N.; Yang, H. Y.; Kim, H. J.; Son, S. U. *Chem. Mater.* **2010**, *22*, 3586.
(24) Wang, Y.; Hu, Y. X.; Zhang, Q. A.; Ge, J. P.; Lu, Z. D.; Hou, Y. B.; Yin, Y. D. *Inorg. Chem.* **2010**, *49*, 6601.
(25) Ithurria, S.; Dubertret, B. *J. Am. Chem. Soc.* **2008**, *130*, 16504.
(26) Manna, L.; Scher, E. C.; Alivisatos, A. P. *J. Am. Chem. Soc.* **2000**, *122*, 12700.
(27) Peng, Z. A.; Peng, X. G. *J. Am. Chem. Soc.* **2001**, *123*, 1389.
(28) Qu, L. H.; Yu, W. W.; Peng, X. P. *Nano Lett.* **2004**, *4*, 465.
(29) Xie, R. G.; Li, Z.; Peng, X. G. *J. Am. Chem. Soc.* **2009**, *131*, 15457.
(30) Pradhan, N.; Reifsnyder, D.; Xie, R. G.; Aldana, J.; Peng, X. G. *J. Am. Chem. Soc.* **2007**, *129*, 9500.
(31) Yu, W. W.; Peng, X. G. *Angew. Chem., Int. Ed.* **2002**, *41*, 2368.
(32) Yang, Y. A.; Wu, H. M.; Williams, K. R.; Cao, Y. C. *Angew. Chem., Int. Ed.* **2005**, *44*, 6712.
(33) Peng, Z. A.; Peng, X. G. *J. Am. Chem. Soc.* **2002**, *124*, 3343.
(34) Li, Z.; Cheng, L. N.; Sun, Q.; Zhu, Z. H.; Riley, M. J.; Aljada, M.; Cheng, Z. X.; Wang, X. L.; Hanson, G. R.; Qiao, S. Z.; Smith, S. C.; Lu, G. Q. *Angew. Chem., Int. Ed.* **2010**, *49*, 2777.
(35) McDaniel, H.; Zuo, J. M.; Shim, M. *J. Am. Chem. Soc.* **2010**, *132*, 3286.
(36) Teranishi, T.; Miyake, M. *Chem. Mater.* **1998**, *10*, 594.
(37) Tsunekawa, S.; Ishikawa, K.; Li, Z. Q.; Kawazoe, Y.; Kasuya, A. *Phys. Rev. Lett.* **2000**, *85*, 3440.
(38) Baumgardner, W. J.; Choi, J. J.; Lim, Y. F.; Hanrath, T. *J. Am. Chem. Soc.* **2010**, *132*, 9519.
(39) David, W. I. F. *J. Appl. Crystallogr.* **1986**, *19*, 63.
(40) Ding, Y.; Wang, Z. L. *J. Phys. Chem. B* **2004**, *108*, 12280.
(41) Fang, C. M.; van Huis, M. A.; Vanmaekelbergh, D.; Zandbergen, H. W. *ACS Nano* **2010**, *4*, 211.
(42) Goldstein, J. *Scanning Electron Microscopy and X-ray Microanalysis*; Kluwer Academic/Plenum Publishers: New York, 2003.
(43) Nakamoto, K. *Infrared and Raman Spectra of Inorganic and Coordination Compounds Part B, Applications in Coordination, Organometallic, and Bioinorganic Chemistry*; John Wiley and Sons: Hoboken, NJ, 2009; pp 64−67.
(44) Bronstein, L. M.; Huang, X. L.; Retrum, J.; Schmucker, A.; Pink, M.; Stein, B. D.; Dragnea, B. *Chem. Mater.* **2007**, *19*, 3624.
(45) He, J. B.; Kanjanaboos, P.; Frazer, N. L.; Weis, A.; Lin, X. M.; Jaeger, H. M. *Small* **2010**, *6*, 1449.
(46) Ouyang, J.; Zaman, M. B.; Yan, F. J.; Johnston, D.; Li, G.; Wu, X.; Leek, D.; Ratcliffe, C. I.; Ripmeester, J. A.; Yu, K. *J. Phys. Chem. C* **2008**, *112*, 13805.
(47) Wang, R. B.; Ouyang, J. Y.; Nikolaus, S.; Brestaz, L.; Zaman, M. B.; Wu, X. H.; Leek, D.; Ratcliffe, C. I.; Yu, K. *Chem. Commun.* **2009**, 962.
(48) Vossmeyer, T.; Katsikas, L.; Giersig, M.; Popovic, I. G.; Diesner, K.; Chemseddine, A.; Eychmuller, A.; Weller, H. *J. Phys. Chem.* **1994**, *98*, 7665.
(49) Li, Z.; Xie, R. G.; Grisham, S. Y.; Peng, X. G., unpublished results.
(50) Jones, G.; Jackson, W. R.; Choi, C.; Bergmark, W. R. *J. Phys. Chem.* **1985**, *89*, 294.